Instability phenomena and their control in statics and dynamics: Application to deep and shallow truss and frame structures

Rosa Adela Mejia-Nava[*1], Adnan Ibrahimbegovic[1a] and Rogelio Lozano-Leal[2]

[1]Université de Technologie Compiégne, Laboratoire Roberval of Mechanics, France
[2]Université de Technologie Compiégne, Heudiasyc UMR CNRS 7253, France

Abstract. In this paper we study the control for nonlinear geometric instability problem of a deep or a shallow truss or yet a frame structure. All the structural models are built with geometrically exact truss and beam finite elements. The proposed models can successfully handle large overall motion under static or dynamic conservative load. The control strategy considers adding a damping from either friction device or viscous damper. This kind of control belong to well-known concept of passivity. Different examples are presented in order to illustrate the proposed theoretical developments.

Keywords: instability; control; viscous damping; friction damping

1. Introduction

The design of a structural systems involves many parameters that influence the response of the structure under conservative static or dynamic loads. For the optimal result for the design close to reality, it is very important to know how to detect the presence of instabilities, and to solve any such problem for preventing the structure collapse. Most of the instability problems such as Euler buckling have been studied under a conservative load and small pre-buckling displacement. Much less is known on nonlinear instability that is characterized by large overall motion, and in particular very large pre-buckling displacements. Gaining a better insight in non-linear instability the goal of this paper is the study of instability of structures in dynamic framework, which has not been studied sufficiently especially on how to control instability-induced vibrating. More precisely to avoid instability of structure or to be able to control it under dynamic loads, can be achieved by adding a damping provided by some kind of external damping mechanism. One can use a viscous damper, a friction device or a smart shape memory alloy (Oliveira *et al.* 2017 and Machado *et al.* 2009).

Any control of this kind is equivalent to the well-known concept of passivity (e.g., see Brogliato *et al.* 2008). This paper presents an application of the finite element method to solving such instability problem with large overall displacements of elastic truss and frame structures, subject to a conservative force. Different ways to achieve the passive control are discussed for nonlinear instability problem for a shallow two-dimensional elastic truss and frame structure.

---

*Corresponding author, Ph.D. Student, E-mail: rosa-adela.mejia-nava@utc.fr
[a]Professor, E-mail: adnan.ibrahimbegovic@utc.fr
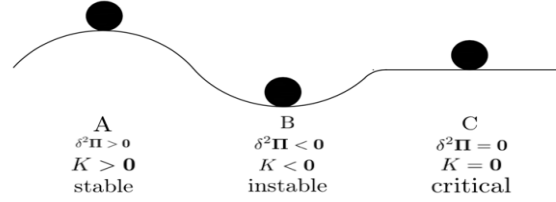
Fig. 1 Energy criteria of instability

The outline of the paper is as follows. Different criteria for detecting instability are presented in Section 2. In Section 3 we discuss different types of instability phenomena, illustrated on a geometrically nonlinear truss structure. In section 4 we introduce geometrically exact beam model, with both linear and nonlinear instability problems. The dynamic framework with different ways of instability control, including viscous damping or friction devices, are presented in Section 5. Several illustrative numerical examples are presented in Section 6. In section 7, we give some conclusive remarks.

2. Instability phenomena: linear versus nonlinear buckling

The instability phenomena imply in general that a small perturbation of loading can lead to a disproportional amplification of the response. The instability depends on many factors, such as the nature of load, the spatial geometry, the material properties, boundary conditions like connections and supports, as well the mass (see Ibrahimbegovic 2009, Argyris and Symeonidis 1981, Simitses and Hodges 2006, Xu *et al.* 2018).

2.1 Detection criteria for instability in statics

Contrary to linear instability (see Fig. 1) the pre-buckling displacement for nonlinear instability is very large. Hence, such problem solution requires the full power of the nonlinear formulation and solution method.

2.1.1 Energy criteria
For the class of conservative problems, the instability of an equilibrium state can be evaluated by the second variation of total the potential energy, which can be written as

$$\delta\Pi(u + \alpha w) = \Pi(u) + \delta\Pi(u; w) + \frac{1}{2}\delta^2\Pi(u; w) + O(\|\delta u\|^2) \tag{1}$$

For illustration, we look at a simple conservative system of the body in the gravity field with three different positions (see Fig. 1). For positon B, if the body is disturbed for a small disturbance, it will simply oscillate around the static equilibrium position, and this position is called stable. The second derivative of the total potential energy for this position remains positive. If the body is disturbed at point A, it will tend to move away from the static equilibrium position; and such an equilibrium position is called unstable. In this case, the second derivative of the total potential energy is negative. Finally, if the body is disturbed at point C, it will tend to remain in disturbed position and the value of the second derivative of the total potential energy is equal to zero; such equilibrium

point regarding from state to unstable equilibrium is referred to as critical (see Ibrahimbegovic 2009, Simitses and Hodges 2006).

2.1.2 Criteria based on singularity of stiffness Matrix

The energy criterion can also be restated in terms of the stiffness matrix. Namely, when the tangent stiffness matrix becomes singular, its determinant takes zero value at the critical state of equilibrium.

$$\delta^2 \pi(\delta u; \delta u) = \delta u^T K \delta u = 0 \Rightarrow det\big[\widehat{K}(d_{cr})\big] = 0 \tag{2}$$

Due to excessively high computing cost of the determinant of the stiffness matrix and rapid increase/decrease in values of the determinant around zero can lead to significant convergence difficulties of Newton's iterative method for computing the corresponding displacement. Thus the determinant-based criterion for detection of the critical equilibrium state is not very practical (see Ibrahimbegovic 2009).

2.1.3 Criteria based on zero eigenvalue

Criterion based on zero eigenvalue reveals instability in terms of the corresponding zero eigenvalue. Such criterion not only can be used to verify if the tangent stiffness is a singular matrix, but also with this detection criterion we can indicate the type of instability mode by computing the eigenvector of the tangent stiffness at the critical equilibrium point associated with zero eigenvalue. The transition of the structure from stability to instability occurs with a zero-eigenvalue (see Argyris and Symeonidis 1981 and see Ibrahimbegovic 2009)

$$[K - \lambda_{cr} I]\psi_{cr} = 0 \Rightarrow K\psi_{cr} = 0 \tag{3}$$

3. Instability computation for truss structures

3.1 Criteria based on zero eigenvalue for linear instability

For the special case, of small pre-buckling displacements the tangent stiffness can be expressed in a simplified form, where the geometric part of the tangent stiffness is a linear function of applied loading (Ibrahimbegovic *et al.* 2013). For example, for a simple structure that consists of 2 truss-bar elements, (see Fig. 3) the present case of geometric instability, the critical values can be obtained as

$$det\big[K_m + \lambda_{cr} K_g\big] = 0 \;\Rightarrow\; \frac{2EA}{l^3}\frac{h^3}{b^2}\left(b^2 + hu_{cr} + \frac{1}{2}u_{cr}^2\right) = 0 \tag{4}$$

where the material and geometric part of the stiffness matrix can be written as

$$K_m^e = \frac{EA}{l^e}\begin{bmatrix} 1 & 0 & -1 & 0 \\ 0 & 0 & 0 & 0 \\ -1 & 0 & 1 & 0 \\ 0 & 0 & 0 & 0 \end{bmatrix} \; ; \; K_g^e = \frac{N}{l^e}\begin{bmatrix} 0 & 0 & 0 & 0 \\ 0 & 1 & 0 & -1 \\ 0 & 0 & 0 & 0 \\ 0 & -1 & 0 & 1 \end{bmatrix} \tag{5}$$

By improving the boundary conditions and solving the resulting eigenvalue problem, we can finally obtain, the values of the critical load as

$$\lambda_{cr1} = \frac{E2A}{l^e}\frac{b^2}{h} \; ; \; \lambda_{cr2} = \frac{E2A}{l^e}\frac{h^3}{b^2} \tag{6}$$
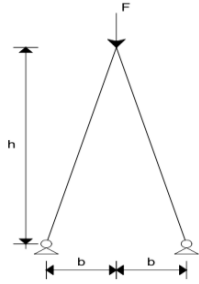
Fig. 2 Deep truss structure
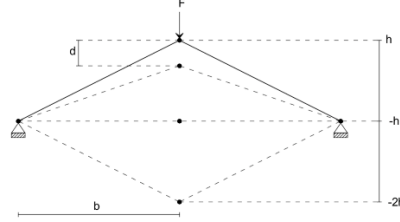
Fig. 3 shallow truss structure

We can express the critical displacement as function of the geometric characteristics of the truss structure as

$$u_{cr} = -h \pm \sqrt{h^2 - 2b^2} \tag{7}$$

We note that these values of the critical displacement are only possible for deep truss (*b<<h*, see Fig. 2), and more importantly they lead to small pre-buckling displacement

3.2 Nonlinear instability

In the class of problems referred to as nonlinear instability, all the displacements, rotations and strains are all large in general before arriving at the critical equilibrium point. For that reason, it is often impossible to obtain the analytic solution, as the one available for linear instability problem of Euler´s buckling (see Ibrahimbegovic 2009). One exception is a general problem in nonlinear instability for a shallow truss composed of two truss-bar elements with 2-nodes, which is loaded by a vertical force at the apex. We can note that maintaining the stability of equilibrium in the system will require zero value of vertical external force for the displacement values *v=h* and *v=2h*. These two equilibrium states correspond, respectively, to the truss equilibrium state where both bars are horizontal and the equilibrium state where bars have been moved through to the opposite side so that the deformed length of each bar remains the same as in the initial configuration, which implies zero internal force.

The natural deformation measure for such truss is the stretch, which can be computed as the ratio of the deformed versus initial length of the bar

$$\lambda_t = l_t^\varphi / l \tag{8}$$

4. Instability computation for frame structure

For the computational purpose, it is better to use the Green–Lagrange strain, which can be easily computed for a 2-node truss bar element as

$$E_{11}^h \big|_l = \frac{1}{(l)^2} x^{eT} H^e d^e + \frac{1}{2(l)^2} d^{eT} H^e d^e \tag{9}$$

Where x^{eT} are nodal coordinates d^e nodal displacements and H^e has block unit matrix structure that means

$$H^e = \begin{bmatrix} I & -I \\ -I & I \end{bmatrix} \tag{10}$$

When the truss constitutive behaviour is linear elastic, which means it is governed by the Saint-Venant–Kirchhoff material law, we can easily obtain the corresponding finite element approximation of the second Piola-Kirchhoff stress as

$$S_{11}^h\big|_l = E \left(\frac{1}{(l)^2} x^{eT} H d^e + \frac{1}{2(l)^2} d^e H d^e \right) \tag{11}$$

Where E is Young's module.

We can also obtain the corresponding finite element approximation of the virtual Green–Lagrange strain

$$\Gamma_{11} = \frac{1}{(l)^2} \left(x^{eT} + d^{eT} H w^e \right) ; \quad w^e = \begin{pmatrix} w_{1,1}^e \\ w_{1,2}^e \\ w_{2,1}^e \\ w_{2,2}^e \end{pmatrix} \tag{12}$$

Where w^e are nodal values of virtual displacements.

Finally, the contribution to the discrete approximation allow us to define the internal virtual work according to

$$G^{int,e} = w^T f^{int,e} ; \quad f^{int,e} = H^T \frac{1}{l} (x^e + d^e) S_{11}^h \tag{13}$$

where we denote

$$x^e = \begin{pmatrix} x_1 \\ y_2 \\ x_2 \\ y_2 \end{pmatrix} ; d^e = \begin{pmatrix} d_{1,1}^e \\ d_{1,2}^e \\ d_{2,1}^e \\ d_{2,2}^e \end{pmatrix} ; H^e = \begin{pmatrix} 1 & 0 & -1 & 0 \\ 0 & 1 & 0 & -1 \\ -1 & 0 & 1 & 0 \\ 0 & -1 & 0 & 1 \end{pmatrix} \tag{14}$$

Introducing the consistent linearization of this week form, we obtain the tangent stiffness matrix, with the material and geometric part that can be written as

$$K^e = K_m^e + K_g^e \tag{15}$$

By assuming the motion symmetry, the weak form of the equilibrium equations for this shallow truss structure can be rewritten as

$$G^{ext} = G^{int} \Leftrightarrow wf = w2AS_{11} \frac{1}{l}(h+v) ; S_{11} = E \frac{1}{l^2} \left(hv + \frac{1}{2} v^2 \right) \tag{16}$$

which allows us to define the explicit form of internal force as a function of (the only non-zero component) of vertical displacement v

$$f = \frac{2EA}{l^3} (h+v) \left(hv + \frac{1}{2} v^2 \right) \tag{17}$$

The corresponding tangent stiffness matrix also reduces to a single entry. This, it is easy to confirm the presence of two critical equilibrium states, which can be computed from zero value of K

$$0 = K := \frac{df^{int}}{dv} = \frac{2EA}{l^3} (h+v)^2 + \frac{2EA}{l^3} \left(hv + \frac{1}{2} v^2 \right) \tag{18}$$
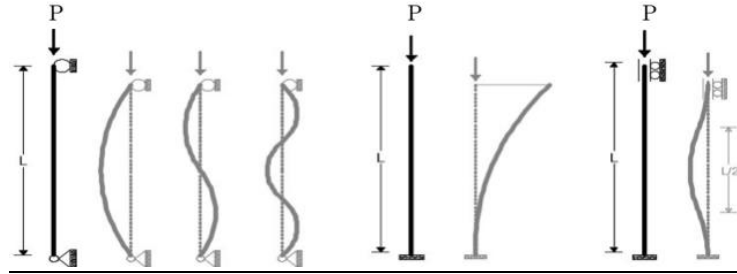
Fig. 4 Euler's buckling. (a) Simple supported (b) One fixed-one free end (c) Both end fixed beam

The classical example of linear geometric instability is Euler's buckling (see Fig. 4), which assumes small pre-buckling displacements. Namely we consider an ideal column assumed initially to be perfectly straight and submitted at the top to the compressive axial load *P*. A small transverse perturbation is applied producing small pre-buckling displacement in terms of a small deflection. If the load *P* is smaller than the critical value, no buckling will happen and the column will remain straight once the perturbation is removed. We define the critical load as the axial load sufficient to keep the bar in a slightly bent form, and producing disproportionality large transverse displacement for any further, even small increase.

The critical equilibrium point of this kind is referred to as bifurcation (see Ibrahimbegovic 2009), Simitses and Hodges 2006, Chen and Lui 1987). The critical force for Euler's beam can be calculated by solving differential equation that corresponds to beam equilibrium. The Euler solution method enabled us to reduce the problem of instability to a simpler problem of finding the minimum characteristic value of the corresponding boundary-value problems (Simitses and Hodges 2006).

$$\frac{d^2y(x)}{dx^2} + \frac{p}{EI}y(x) = 0 \tag{19}$$

The general solution of this ordinary equation can be written as

$$F_{cr} = \frac{\pi^2 EI}{cl^2}; y = A\cos kx + B\sin kx \tag{20}$$

where *c* is the constant that depend, on boundary conditions, whereas *A* and *B* are constants defining the instability mode. If we solve this equations for each particular boundary condition, we will be able to find the critical load (see Fig. 4 for different cases).

$$F_{cr} = \frac{n^2\pi^2 EI}{l^2} \tag{21}$$

$$F_{cr} = \frac{\pi^2 EI}{4l^2} \tag{22}$$

$$F_{cr} = \frac{2{,}05\pi^2 EI}{l^2} \tag{23}$$

4.1 Nonlinear instability of geometric exact beam model: large pre-bucling displacements and rotations

As possible enhancement of the truss model, we can use geometrically exact beam instead of the truss (see Ibrahimbegovic 1997, Ibrahimbegovic and Frey 1993, Imamovic *et al.* 2018). This time, the instability phenomena can be present in both large displacement and large rotations setting of geometrically nonlinear problems. When a deformable beam is submitted to large displacements, large rotations and large deformations, the initial configuration at the beginning of a given loading program and the deformed configuration at the end are quite different, such as in the case of a shallow beam after to be submitted to the critical load.

The generalized strain measures proposed by Reissner (e.g., Ibrahimbegovic 1995) are expressed as function of the rotation matrix Λ, position vector φ and unit vector e_1 as

$$\begin{pmatrix} E \\ \Gamma \end{pmatrix} = \Lambda^T \varphi' - e_1 \; ; \;\; K = \frac{d\psi}{dx} \tag{24}$$

For 2*d* case, the rotation matrix and position vector are written as

$$\Lambda = \begin{bmatrix} \cos\psi & -\sin\psi \\ \sin\psi & \cos\psi \end{bmatrix} \; ; \;\; \varphi' = \frac{d}{dx}\begin{pmatrix} x+u \\ v \end{pmatrix} \tag{25}$$

Therefore, the generalized strain measures can be expressed as

$$\begin{aligned} E &= \cos\psi \left(\frac{dx}{ds} + \frac{du}{ds} \right) + \sin\psi \left(\frac{dy}{ds} + \frac{dv}{ds} \right) - 1 \\ \Gamma &= -\sin\psi \left(\frac{dx}{ds} + \frac{du}{ds} \right) + \cos\psi \left(\frac{dy}{ds} + \frac{dv}{ds} \right) \\ K &= \frac{d\psi}{dx} \end{aligned} \tag{26}$$

The virtual work can be expressed in terms of non-symmetric Piola-Kirchhoff stress *P* and its energy conjugate strain measure as the deformation gradient *F*.

$$G(u; w) = \int_L \int_A \hat{F} * P \, dA \, ds - \int_L w^T f \, ds = 0 \tag{27}$$

The virtual work can be restated in terms of stress resultants as follow (see Ibrahimbegovic and Frey 1993)

$$G(u; w) = \int_L \langle d^T(w)\Lambda + \hat{\psi} h^T(a)\frac{d\Lambda}{d\psi} \rangle r \, ds - \int_L w^T f \, ds = 0 \tag{28}$$

All the instability criteria already by the truss model are also valid for this geometrically exact beam model, for the case of conservative loading where we can define the potential energy.

5. Dynamic framework and time-integration schemes

For the case where total potential energy cannot be defined (for a e.g., non-conservative loading, follower force), we can switch to dynamic frame work for instability (Hemat *et al.* 2018, Mohammad *et al.* 2019). In general case, the dynamics equations are solved by using time integration schemes.

The instability criteria already presented by the truss model are all valid for this geometrically exact beam model, for the case of conservative loading where we can define the total potential energy. The solution of the differential equation of motion can be obtained through numerical methods with step-by-step time integration scheme. The solution depend on initial conditions, and

has to include the equations of motion at time t_{n+1}.

$$M\ddot{d}_{n+1} + C\dot{d}_{n+1} + Kd_{n+1} = F_{n+1}^{ext} \tag{29}$$

The best solution can be obtained by the second-order time-integration schemes, such as the central difference or the Newmark method. In this work, we can work with either the first or the second method, where the velocity and displacement can be expressed as

$$d_{n+1} = d_n + h\dot{d}_n + h^2\left[\left(\frac{1}{2} - \beta\right)a_n + \beta a_{n+1}\right]$$
$$\dot{d}_{n+1} = \dot{d}_n + h\left[(1 - \gamma)\ddot{d}_n + \gamma\ddot{d}_{n+1}\right] \tag{30}$$

Here, the factor γ affects, the acceleration in the velocity equation, whereas β affects displacements. With values β equal to 0 and γ equal 1/2 we obtain the central difference and with values $\beta=1/4$ and $\gamma=1/2$ correspond to the trapezoidal rule, which assumes that acceleration will remain constant (see Ibrahimbegovic 2009, Clough and Penzien 1993, Chapra and Canale 2015).

The dynamic response of a simple dynamic system can oscillate indefinitely if it does not have any force that can dissipate energy and reduce motion to zero. However, in real life the oscillation will reduce gradually due to damping of the system. Here, we present two types of damping, which both fit into the same framework.

$$f^{int}(d) + damping = f^{ext} \tag{31}$$

5.1 Viscous damping

This model is used successfully to model the exponential vibration amplitude decay in a variety of mechanical systems. One example of viscous damper can be a piston fit into a cylinder filled with oil. Here the damping force is proportional to the velocity of the piston, in direction opposite of the motion. Such a damping force illustrated in Fig. 5 has the form

$$f_c = c\dot{d}(t) \tag{32}$$

5.2 Frictional damping

This kind of damping with sliding friction is well known Coulomb damping, which is characterized by
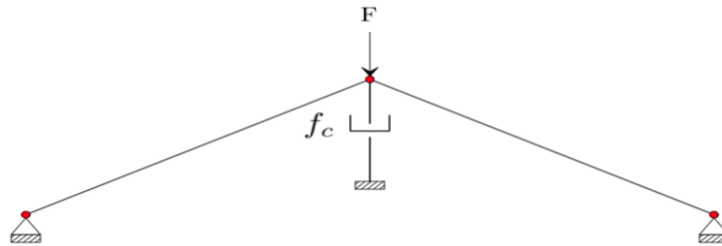

Fig. 5 Viscous damping
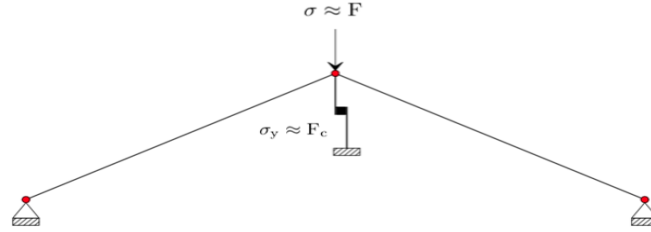
Fig. 6 Model perfect plasticity

$$f_c(\dot{d}) = \begin{cases} -\mu N & \dot{d} > 0 \\ 0 & \dot{d} = 0 \\ \mu N & \dot{d} < 0 \end{cases} \tag{33}$$

One way to illustrate this kind of damping in a system shown in Fig. 6, It is equivalent to perfect plasticity model where the sliding resistance is equal to elasticity limit σ_y (see Ibrahimbegovic 2009, Inman 2014).

Finally, such damping modifies the equation of motion as expressed in the following way

$$M\ddot{d} + f_c sgn(\dot{d}) + f^{int}(d) = f^{ext} \tag{34}$$

In short, adding different damping mechanism correspond to passive control of vibration (see Lozano and Brogliato 1992, Lozano *et al.* 2008)

Passive control of vibrations was used successfully in many control applications, for example, the stabilization of unmanned aerial vehicle using unit quaternions (see Guerrero-Sanchez *et al.* 2016) where the authors reduced the problem to the longitudinal plane and the potential energy *V=mgz*, as a conservative load by the product of the mass m, gravity *g*, and the position in the vertical axis in the internal frame *z*:

Hence, to design structures or machines and have a desired transient and steady state response to some extent the designer can play with mass, stiffness or damping. Adding mass and changing stiffness values are also methods of passive control. However, it is not always possible to choose all the parameters to play with them due to design constraints that have to be satisfied. Hence, in order to avoid vibrations, it may be necessary to add an external damper or some mass could be added to a given structure to lower its natural frequency. Damping treatments increase the rate of decay of vibrations as the nonlinear control technique based on passivity. Passivity is a fundamental property exhibited by many physical systems which involves energy dissipation and transformation (see Inman 2006).

6. Numerical examples

In this section, we present several illustrative numerical examples of instability computations and control. First example is a simple cantilever beam in free vibration represented, with a truss element, where we control the beam vibrations by adding two different kinds of damping in order to dissipate the oscillations, viscous damping and equivalent friction damping, in order to dissipate the oscillations. Then we consider the case of a nonlinear instability case with the Williams toggle
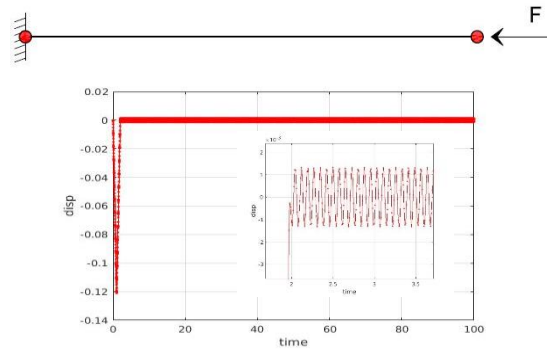
Fig. 7 Oscillations Cantilever truss
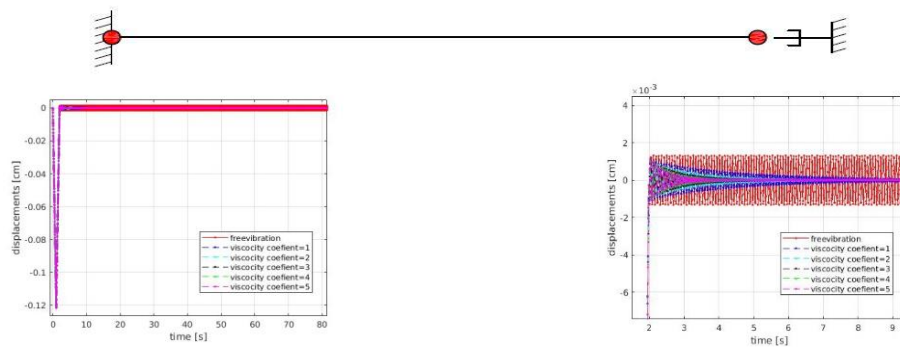
Fig. 8 (a) Cantilever truss with viscous damping, (b) oscillations changing viscosity coefficient

frame which is modelled with either two truss elements for 8 beam elements. In the first case, we will present arc-length method results and after that the results, we obtain by adding viscous damping and equivalent friction damping.

6.1 Simple cantilever with truss element

We propose control of axial oscillations of a simple cantilever modeled by truss in order two different a simple cases of vibration control and show how the structure will behave. We take a cantilever first subjected to a triangular pulse load, which will continue to oscillate in free vibration (see Fig. 7). The chosen material and geometric characteristics are $EI=2.66\times10^5$ Ncm^2, $EA=8.251\times10^6$ N, $\rho=7.79\times10^{-3}$ kg/cm^3.

For dissipating these oscillations, we can use two kinds of damping, which is modelled with special elements placed at the end of the bar. The first one is viscous damping, which depends on the viscosity coefficient, and the second is a friction damping, which depends on frictional coefficient.

6.1.1 Cantilever truss element with viscous damping

In the case when we add a viscous damping, the cantilever oscillation will decrease, with decrement that depends on the value of the viscosity coefficient. If we further increase this value, the amplitude of oscillations decay time will be shorter (see Fig. 8).

(a) displacement-time

(b) displacement-time zoom
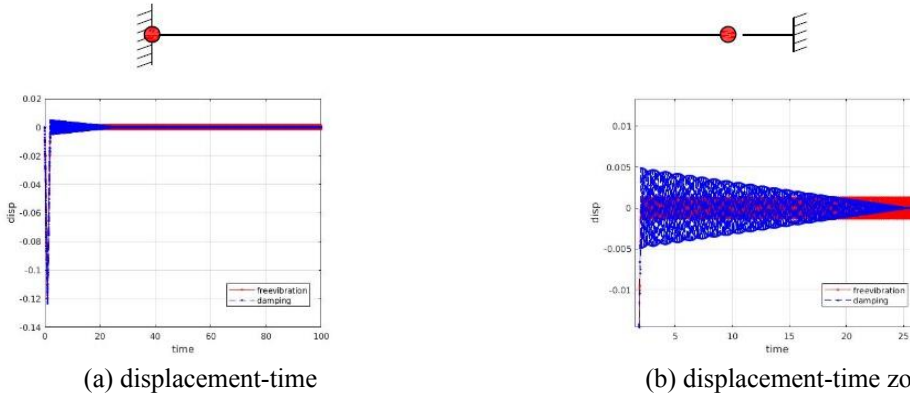
Fig. 9 Cantilever truss, oscillations displacement-time of free vibration and friction damping

(a) displacement-time

(b) displacement-time zoom
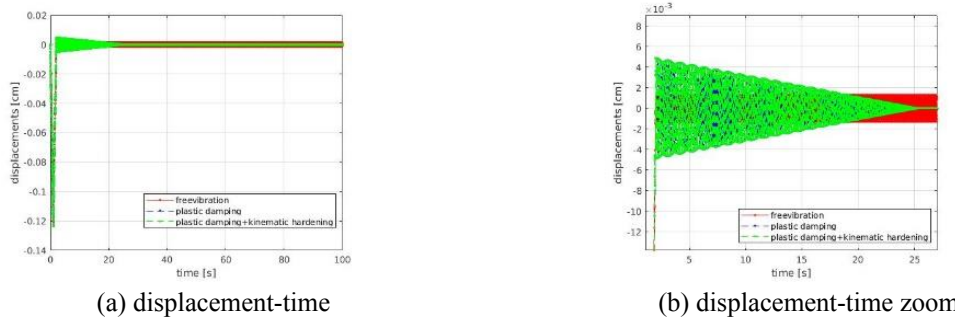
Fig. 10 Cantilever truss, oscillations displacement-time of free vibration, friction damping and kinematic hardening
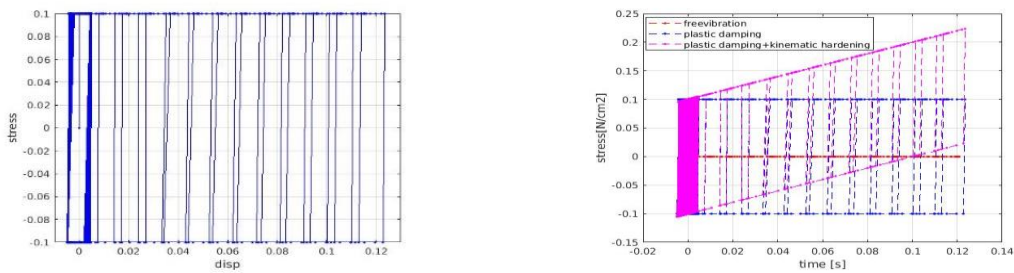
(a) stress-displacement perfect plasticity (friction damping)

(b) stress-displacement perfect plasticity (friction damping) and kinematic hardening

Fig. 11 Cantilever truss, stress-displacement of free vibration, perfect plasticity and kinematic hardening

6.1.2 Cantilever truss element with friction damping

For the second option of vibration control we take the same cantilever truss, and we add a friction element at free end (see Fig. 9), we propose an equivalent friction damping. The first control model is a truss element with perfect plasticity, and the second one is plasticity with kinematic hardening. We note that these models are not exactly pure friction. However, they can still store dissipate energy, since the rheological model of plasticity consists of elastic plus friction part.
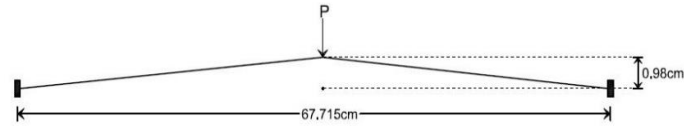
Fig. 12 Geometry and load conditions of toggle frame
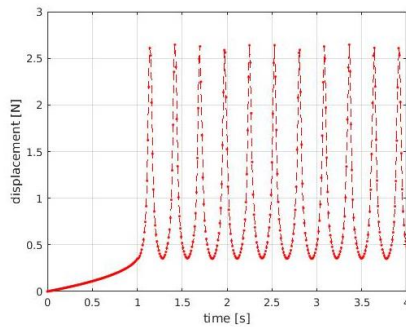
(a) Truss elements free vibration
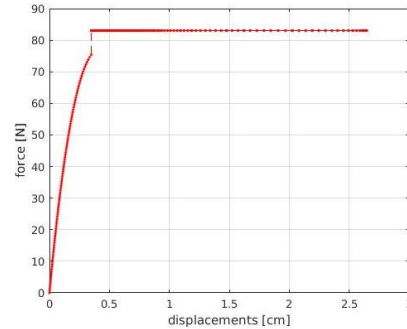
(b) Truss elements free vibration oscillation

Fig. 13 Diagram force displacement truss element
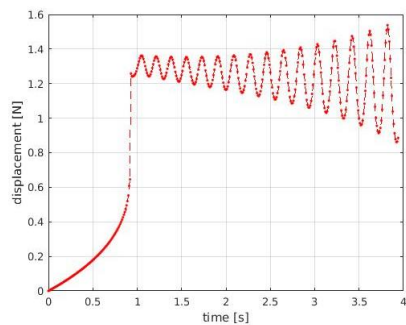
(a) Beam element free vibration
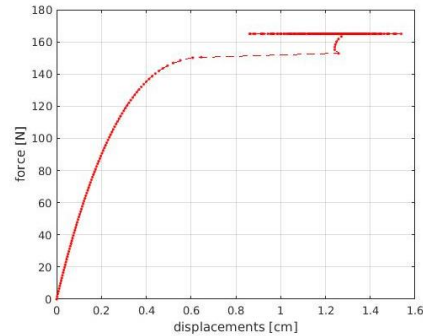
(b) Beam element free vibration oscillation

Fig. 14 Diagram force displacement beam element

6.2 Williams toggle frame

In this section we present a vibration control example of William toggle frame one, with truss elements and other with beams (see Fig. 12). This example considers the nonlinear instability. This frame consists of two legs each supported on one end and on the other loaded by a vertical force at the apex. The chosen material characteristics are EI=2.66×10^5 Ncm^2, EA=8.251×10^6 N, ρ=7.79×10^{-3} kg/cm^3. A numerical solution is presented in Mamouri *et al.* (2015).

When increasing the values of applied load, the frame displacement increases proportionally until the load reaches the critical value. At critical load, the sudden increase of displacement will occur. In computing this first part of response, we perform the static analysis. Subsequently we continue with the dynamic analysis, where we apply the Newmark time integration scheme (see Figs. 13 and 14). We present two different models of this structure: first with two truss elements
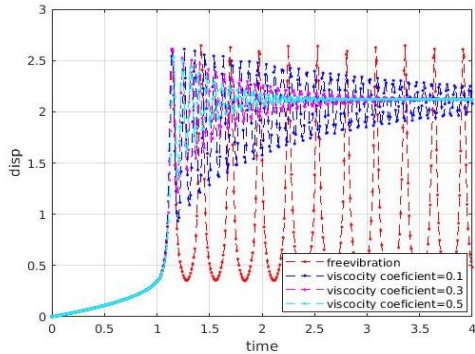
(a) Diagram force displacement
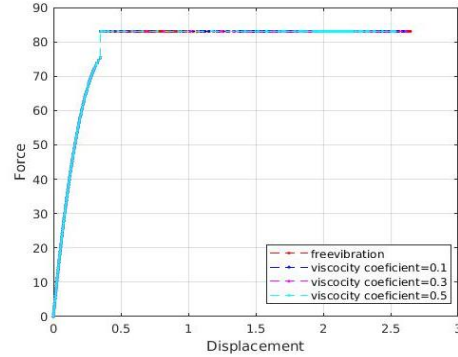
(b) Diagram force displacement oscillation

Fig. 15 Williams toggle frame modelled with truss elements with viscous damping
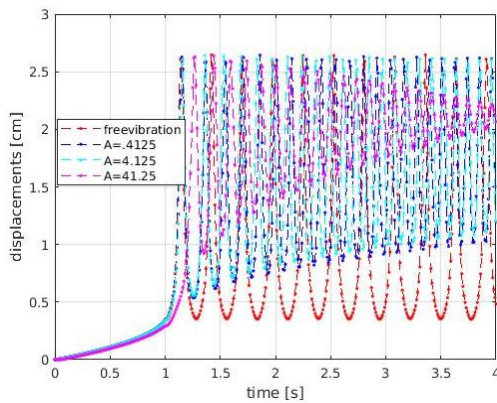
(a) Diagram force displacement
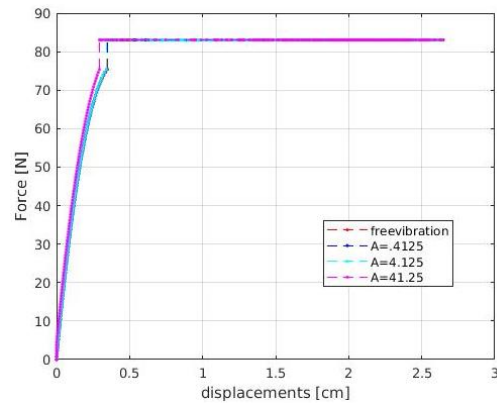
(b) Diagram force displacement oscillation

Fig. 16 Williams toggle frame modelled with truss elements with perfect plasticity damping

and second with 8 beam elements.

At the end of instability induced sudden jump in dynamics we will see some oscillations (see Fig. 13(b) and 14 (b)), and the goal will be to damp out these oscillations. Thus we propose to first add a viscus damping and then to add an equivalent friction damping like in the case of cantilever beam.

6.2.1 Williams toggle frame model with truss elements

In this part we model the frame with two truss elements chosen material with the properties and geometry shown in Fig. 12. First we add viscous damping and then an equivalent friction damping, with a perfect plasticity. We check their ability to control oscillations after the critical load.

In the first case when we add a viscous damping the behavior is similar to the cantilever truss. Namely, the decay of vibration amplitude directly depends on viscosity coefficient. The oscillations will decrease faster when we increase this value. For the case of perfect plasticity, we change area values. The oscillations are changing directly with changing this value. The values in this analysis were chosen as .4125, 4.125 and 41.25 of the cross section of the damping device. We can see the results in Fig. 16. With the value of .425, the amplitude of oscillations decreases but is not meaningful. Here the value that dissipates energy is 41.125. We change this area in the function of the area of the frame element.
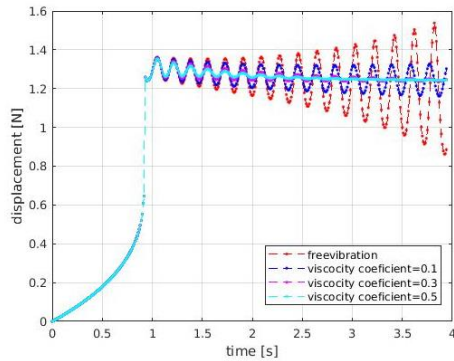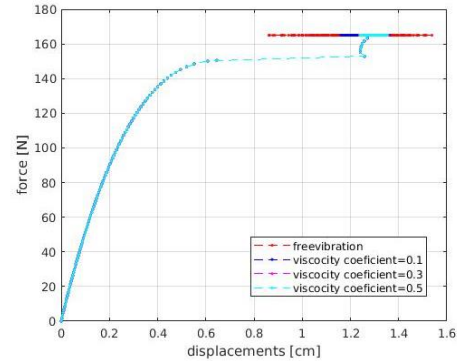
(a) Diagram force displacement   (b) Diagram force displacement oscillation

Fig. 17 Williams toggle frame modelled with beam elements with viscous damping
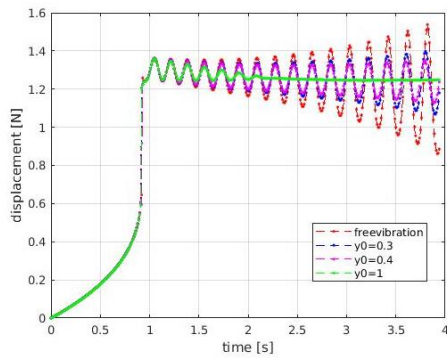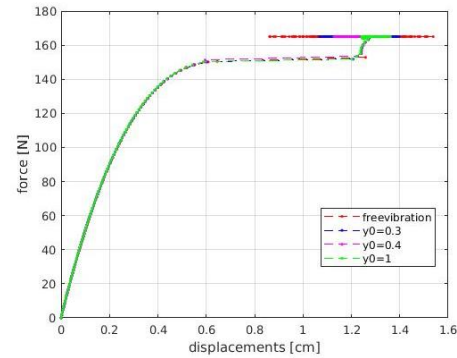
(a) Diagram force displacement   (b) Diagram force displacement oscillation

Fig. 18 Williams toggle frame modelled with beam elements with perfect plasticity damping

6.2.2 Williams toggle modelled with frame beam elements

Here, we model the frame with 8 beam elements. We use the same properties as shown in Fig. 12. Again we use viscous damping and equivalent friction damping with either perfect plasticity or another one with kinematic hardening.

With these elements, the behavior is similar to the previous two when we add viscous damping, as the viscosity coefficient increases the dissipation also increases until one point where there are no oscillations. On the other hand, for plastic damping the key factor is the chosen value of the yield stress. The oscillations are changing directly with changing this value. The values in this analysis were chosen as 0.3, 0.4 and 1. We can see the results in Fig. 18.

7. Conclusions

We have presented different criteria for nonlinear instability problem, and corresponding illustrative examples. A shallow beam under a static load in the apex will be unstable after the critical load. If after the critical load we continue the analysis in dynamics the structure will start to oscillate. One way to control this oscillation is by adding either viscous damping or friction damping. In

nonlinear instability under dynamic load, we implement two different kinds of damping mechanism (viscous damping and friction damping) for verifying the dissipative behavior.

When we add viscous damping to the truss structure and William toggle frame the reduction of oscillations depends of the viscous damping coefficient, if we increase this value we will obtain a reduction of the oscillations. Equivalent friction damping with perfect plasticity behavior is more particular for each case. For example, in the case of the truss in cantilever dissipation depends on the yield stress, as well as in the in the case of beam William Toggle frame. However, for the William toggle frame with truss elements dissipation depend on area of the devise, greater area greater dissipation.

In future developments we plan to generalize the proposed approach to the case of non-conservative loading, such as those produced by fluids pressure brought by wind loads (e.g., Ibrahimbegovic and Boujelben 2018); the latter requires rather special treatment (Bolotin 1963) within the proposed dynamics framework. We also plan to generalize to using this approach for practical application, such as planned destruction of an existing building (e.g., El Houcine *et al*. 2018).

Acknowledgments

References

Abolfazl, J.N., Gholamreza, S.J. and Reza, K. (2018), "Vibration and instability of nanocomposite pipes conveying fluid mixed by nanoparticles resting on viscoelastic foundation", *Comput. Concrete*, **21**, 569-582. https://doi.org/10.12989/cac.2018.21.5.569.

Argyris, J.H. and Symeonidis, S. (1981), "Nonlinear finite element analysis of elastic systems under nonconservative loading-Natural formulation. Part I. Quasistatic problems", *Comput. Meth. Appl. Mech. Eng*., **26**(l), 75-124. https://doi.org/10.1016/0045-7825(81)90131-6.

Bolotin, V.V. (1963), *Fundamentals of Structural Stability*, Pergamon.

Brogliato B., Lozano, R., Maschke, B. and Egeland, O. (2008), *Dissipative Systems Analysis and Control*, Springer Series in Communications and Control Engineering.

Chapra, S.C. and Canale, R.P. (2015), *Numerical Methods for Engineers*, McGraw-Hill.

Chen, W.F. and Lui, E.M. (1987), *Structural Stability*, Elsevier

Clough, R.W. and Penzien, J. (1993), *Dynamics of Structures*, McGraw-Hill.

El Houcine, M., Mamouri, S. and Ibrahimbegovic, A. (2018), "A controlled destruction and progressive collapse of 2D reinforced concrete frame", *Coupl. Syst. Mech.*, **7**, 111-139. https://doi.org/10.12989/csm.2018.7.2.111.

Guerrero-Sanchez, M.E., Abaunza, H., Castillo, P., Lozano, R., Garcia-Beltran, C. and Rodriguez-Palacios, A. (2016), "Passivity-based control for a micro air vehicle using unit quaternions", *Appl. Sci.*, **7**(1), 13. https://doi.org/10.3390/app7010013.

Hemat, A.E., Mehran, K. and Morteza, A. (2018), "Dynamic instability response in nanocomposite pipes conveying pulsating ferrofluid flow considering structural damping effects", *Struct. Eng. Mech.*, **68**(3), 359-368. https://doi.org/10.12989/sem.2018.68.3.359.

Ibrahimbegovic, A. (1995), "On finite element implementation of geometrically nonlinear Reissner´s beam theory: three-dimensional curved beam elements", *Comput. Meth. Appl. Mech. Eng.*, **122**, 11-26. https://doi.org/10.1016/0045-7825(95)00724-F.

Ibrahimbegovic, A. (1997), "On the choice of finite rotation parameters", *Comput. Meth. Appl. Mech. Eng.,* **149**, 49-71.

Ibrahimbegovic, A. (2009), *Nonlinear Solid Mechanics*, Spriger.

Ibrahimbegovic, A. and Boujelben, A. (2018), "Long-term simulation of wind turbine structure for distributed loading describing long-term wind loads for preliminary design", *Coupl. Syst. Mech.*, **7**, 233-254. https://doi.org/10.12989/csm.2018.7.2.233.

Ibrahimbegovic, A. and Frey, F. (1993), "Finite element analysis of linear and elastic initially curved beams non-linear planar deformations", *Int. J. Numer. Meth. Eng.*, **36**, 3239-3258. https://doi.org/10.1002/nme.1620361903.

Ibrahimbegovic, A. and Taylor, R.L. (2002), "On the role of frame-invariance in structural mechanics models at finite rotations", *Comput. Meth. Appl. Mech. Eng.*, **191**, 5159-5176. https://doi.org/10.1016/S0045-7825(02)00442-5.

Ibrahimbegovic, A., Hajdo, E. and Dolarevic, S. (2013), "Linear instability or buckling problems for mechanical and coupled thermomechanical extreme conditions", *Coupl. Syst. Mech.*, **2**(4), 349-374. https://doi.org/10.12989/csm.2013.2.4.349.

Imamovic, I., Ibrahimbegovic, A. and Mesic, E. (2018), "Coupled testing-modeling approach to ulitmate state computation of steel structures with connections for statics and dynamics", *Coupl. Syst. Mech.*, **7**, 555-581. https://doi.org/10.12989/csm.2018.7.5.555.

Inman, D.J. (2006), *Vibration with Control*, John Wiley Sons.

Inman, D.J. (2014), *Engineering Vibration*, Pearson Education.

Lozano R., Brogliato, B., Maschke, B. and Egeland, O. (2008), "Passivity-based control system analysis and design", *Springer Series in Communications and Control Engineering*.

Lozano, R. and Brogliato, B. (1992), "Adaptive control of robot manipulators with flexible joints", *IEEE Tran. Auto. Control*, 174-181.

Machado, L.G., Lagoudas, D.C. and Savi, M.A. (2009), "Lyapunov exponents estimation for hysteretic systems", *Int. J. Solid. Struct.*, **46**(6), 1269-1286*. https://doi.org/10.1016/j.ijsolstr.2008.09.013.*

Mamouri, S. and Ibrahimbegovic, A. (1999), "Nonlinear dynamics of flexible beams in planar motion: formulation and time-stepping scheme for stiff problems", *Comput. Struct.*, **70**, 1-22. https://doi.org/10.1016/S0045-7949(98)00150-3.

Mamouri, S., Mourid, E. and Ibrahimbegovic, A. (2015), "Study of geometric nonlinear instability of 2D frame structures", *Eur. J. Comput. Mech.*, **24**, 246-258. https://doi.org/10.1080/17797179.2016.1181028.

Mohammad, A**.**, Mahmoud, P. and Ali, G.A. (2019), "Dynamic instability region analysis of sandwich piezoelectric nano-beam with FG-CNTRCs face-sheets based on various high-order shear deformation and nonlocal strain gradient theory", *Steel Compos. Struct.*, **32**(2), 157-171. https://doi.org/10.12989/scs.2019.32.2.151.

Oliveira, H., De Paula, A.S. and Savi, M.A. (2017), "Study of geometric nonlinear instability of 2D frame structures", *J. Comput. Mech.*, **24**(6), 256-278. https://doi.org/10.1080/17797179.2016.1181028.

Rajesh, K., Tanish, D. and Sarat, K.P. (2019), "Instability and vibration analyses of FG cylindrical panels under parabolic axial compressions", *Steel Compos. Struct.*, **31**(2), 187-199. https://doi.org/10.12989/scs.2019.31.2.187.

Simitses, G.J. and Hodges, D.H. (2006), *Fundamentals of Structural Stability*, Elsevier.

Sofiyev, A.H., Zerin, Z., Allahverdiev, B.P., Hui, D., Turan, F. and Erdem, H. (2017), "The dynamic Instability of FG orthotropic conical shells within the SDT", *Steel Compos. Struct.*, **25**(5), 581-591. https://doi.org/10.12989/scs.2017.25.5.581.

Xu, Y.P., Zheng, Z.L., Liu, C.J., Wu, K. and Song, W.J. (2018), "Aerodynamic stability analysis of geometrically nonlinear orthotropic membrane structure with hyperbolic paraboloid in sag direction", *Wind Struct.*, **26**(6), 355-367. https://doi.org/10.12989/was.2018.26.6.355.